Effect of solution composition on seeded precipitation of calcium for high recovery RO of magnesium-bearing wastewater, surface water or groundwater

Peter Sanciolo*, Stephen Gray

Institute for Sustainability and Innovation, Victoria University, Australia

*Corresponding Author: Tel.: +61 3 9919 8053; fax: +61 3 9919 7696. E-mail address: peter.sanciolo@vu.edu.au; Victoria University, Institute for Sustainability and Innovation, Werribee Campus, P.O. Box 14428, Melbourne, Vic. 8001, Australia

Abstract

The accelerated seeded precipitation (ASP) of calcium salts from simulated municipal wastewater RO brines using calcium carbonate seed is compared to the much more effective but more expensive ASP using calcium phosphate seed. The aim of this study was to identify the test water compositional limitations of ASP using calcium carbonate seed, and to elucidate the chemistry responsible for the different performance of calcium carbonate and calcium phosphate as seed materials in the ASP of calcium from municipal wastewater and magnesium-bearing groundwater.

The results of seeded precipitation of calcium from simulated wastewaters and groundwater with varying composition using $CaCO_3$ seed was found to only be effective in the absence of phosphate and at conditions where the driving force for $MgCO_3$ formation was low. Seeded precipitation using $CaHPO_4$ seed greatly outperformed $CaCO_3$ seeded precipitation at the high carbonate-high magnesium concentration conditions where inhibition was the greatest for $CaCO_3$ seeded precipitation.

SEM images of the seed particles after seeded precipitation showed $CaCO_3$ seeds that appeared to be covered with a thin layer of precipitate. SEM images of the solid formed after $CaHPO_4$ seeded precipitation, however, showed seed that had a thick covering of very small particles.

Keywords: accelerated seeded precipitation; high recovery reverse osmosis; calcium carbonate; calcium phosphate; municipal wastewater, groundwater; magnesium; phosphate; carbonate

1. Introduction

Municipal wastewater and groundwater are valuable water resources for inland locations in Australia at times of water shortage, and play an integral role in sustainable water management strategies of water authorities in inland regions. Due to their salt content, however, their indiscriminate use for irrigation can lead to soil sodicity and crop failure, and many water authorities have included desalination in their strategic plans for the delivery of fit-for-purpose recycled water to their community.

Desalination in inland regions poses a major challenge – the management of the resultant brine concentrate. Extraction of excessive quantities of low salt water from the feedwater during the reverse osmosis (RO) desalination process leads to salt concentrations that are greater than the solubility of certain salts, such as calcium carbonate, calcium sulfate or calcium phosphate, resulting in the formation of mineral scale on the membranes and the reduction in clean water flux through the membranes. To avoid the development of this scale, the recovery of low salt water during the reverse osmosis treatment is kept to values of typically 70% to 80% of the wastewater volume, depending on the wastewater constituent concentrations. The management of the resulting 20% to 30% of the feed volume can be a major burden to the water authority, and represents a major underutilization of the wastewater, particularly at times of drought when wastewater and groundwater resources are called upon more strongly in order to meet the water needs of the community.

Waste brine management and wastewater utilization can be improved by the use of interstage treatment of the RO concentrate to remove scale precursor ions. Interstage treatment involves operating the RO at water recoveries that are not conducive to scale formation, treatment of the resulting RO concentrate to remove the scale precursor ions via precipitation and solid-liquid separation, and then further treating the RO concentrate via another RO stage or by recycling to the feed stream to extract more low salt water. The solid-liquid separation process adopted depends largely on scale and economic considerations. This can be sedimentation and microfiltration as was piloted by Gabelich et al. [1], ceramic filtration as piloted by Sanciolo et al. [2], moving bed filter or any other solid-liquid separation process that can achieve the desired low turbidity (< 1 NTU) for the subsequent RO treatment.

Antiscalants can be added downstream of the ASP stage, i.e. at the second RO stage, as their use in the first stage may hinder the interstage precipitation and removal of scale precursor ions if the ASP process operates at low supersaturation. Alternatively, antiscalant can be added at the first RO stage

and removed by adsorption on $CaCO_3$ seed prior to interstage treatment [3]. In some circumstances, the judicious choice of antiscalant may allow antiscalnt use in the first RO stage without adverse effects in the downstream ASP stage. Sanciolo et al. [2], for example, adopted ASP involving $CaHPO_4$ precipitation on $CaHPO_4$ seed and used an antiscalant that is not effective against $CaHPO_4$ scale formation but is effective against $CaCO_3$ scale formation (Flocon 135) in the first RO stage, thus providing some protection against $CaCO_3$ scale without adversely affecting $CaHPO_4$ precipitation in the ASP stage.

The removal of scale precursors in high recovery RO has been achieved via ion exchange [4], chemical precipitation [1] or seeded precipitation [5]. Interstage demineralization of RO concentrates has been shown to be effective for mildly brackish river water treatment [5, 4] for tap water treatment [6], [7] and for groundwater treatment [8]. Literature studies involving the application of interstage deminerilization to high recovery RO of municipal wastewater, however, are very few [9, 2].

The choice of seed material to be used in ASP is often dictated by the composition of the solution to be treated, with the composition of the seed *usually* being that of the salt to be precipitated. Lin and Singer [10], for example, compared the use of quartz, dolomite and calcite as seed materials for calcium carbonate precipitation from calcium carbonate solution, and found that only calcite had the ability to initiate calcium carbonate precipitation. Similarly, Lioliou et al. [11] investigated seeded precipitation from stable calcium carbonate supersaturated solutions using calcite and quartz seed and found that calcite induced precipitation but quartz did not. The choice of seed material is, however, more difficult when one is dealing with solutions that contain interfering substances. Our earlier work on high recovery RO of municipal wastewaters [2] , that were supersaturated with respect to calcium carbonate, showed that the removal of calcium from the 70% water recovery RO concentrate produced from this wastewater via accelerated seeded precipitation (ASP) using calcium carbonate seedwas not effective. The use of calcium phosphate seed ($CaHPO_4$), however, allowed the reduction of the calcium concentration from 250 mg/L to 10 mg/L. The poor performance of calcium carbonate seed was attributed to the presence of magnesium and phosphate at levels that interfere with the seeded precipitation process [12-24]. The high concentration of calcium, magnesium and phosphate in the wastewater was attributed to the combined effect of high evaporation rate, low flow and groundwater infiltration.

The presence of small quantities of phosphate has been found to markedly slow the precipitation of calcium carbonate from supersaturated solutions [20]. The inhibitory effect of phosphate on calcium carbonate precipitation has been attributed to the chemisorption of aqueous $CaHPO_4$ species [21],

which blocks the active calcium carbonate surface sites, preventing or slowing further calcium carbonate deposition. Similarly, the presence of magnesium ions has been found to retard calcium carbonate precipitation [25] and inhibit calcium carbonate crystal growth [19]. A competitive adsorption model involving Ca^{2+} and Mg^{2+} was found to give a good fit to the experimental data. The inhibitory effect of magnesium ions on unseeded precipitation has also been attributed to the increase in interfacial tension of the newly formed nuclei [16].

Our previous studies of calcium carbonate precipitation in simulated RO brines at pH 10 [26] confirmed the slowing influence of magnesium and phosphate ions on calcium precipitation in the absence of seed, and served to elucidate the solution conditions responsible for calcium carbonate supersaturation in RO brines at this pH. Solutions were equilibrated at pH 10 for 2 hours prior to filtration through 0.45 micron filter and it was found that the filtrate of solutions without magnesium or phosphate had low residual calcium concentrations. The filtrate of solutions containing magnesium had the highest residual calcium concentration. The presence of phosphate on its own was also found to lead to elevated calcium concentrations at the end of the experiment. The combined addition of magnesium and phosphate was found to result in higher residual calcium levels than with these two components added individually. Seeded precipitation experiments using $CaCO_3$ seed also showed that the presence of magnesium and phosphate also significantly affects seeded precipitation of calcium from RO brines.

In this paper, calcium carbonate seeded ASP is tested at different concentrations of magnesium and carbonate, in the presence and absence of phosphate ion, and compared to the much more effective but more expensive ASP using calcium phosphate seed. The aim of this study was to elucidate the test water compositional limitations of interstage ASP using calcium carbonate seed, and the chemistry responsible for the different performance of calcium carbonate and calcium phosphate as seed materials in the ASP of calcium from municipal wastewater and magnesium-bearing groundwater RO concentrates to achieve high RO water recovery.

2. **Methods**

2.1 Seed materials

The particle size of the CaCO$_3$ (Ajax chemicals) and CaHPO$_4$ (BDH chemicals) used as seed were determined using a Malvern Zetasizer Nano-ZS. The powders were dispersed in ASP treated (10 g/L CaCO$_3$ or CaHPO$_4$, pH 10) RO brine that had been filtered through a 0.45 micron cellulose acetate membrane filter. The composition of this RO brine is given in a previous publication [2]. The powders were polydisperse with a high proportion of the particles (>30%) with a diameter larger than 6,000 nm, and exhibiting poor suspension stability. The CaCO$_3$ seed particles with diameters below 6,000 nm were found to have diameters between 13 and 450 nm with the most frequent diameters being between 20 and 250 nm. The CaHPO$_4$ seed particles with diameters below 6,000 nm were found to have diameters between 350 and 2,000 nm with the most frequent diameter being between 600 and 1100 nm. The surface area was determined using a Micromeritics TriStar Surface Area and Porosity analyser to be 0.96 m^2/g for CaCO$_3$ seed and 2.3 m^2/g for CaHPO$_4$ seed.

2.2 Solutions

2.2.1. Seeded precipitation trials

The solution magnesium, phosphate and carbonate concentrations used are shown in Table 1. The solution Mg^{2+} : Ca^{2+} ratio and CO$_3^{2-}$: Ca^{2+} ratio are shown in Table 2. Ten millilitre aliquots of the required stock salt solutions were delivered to a 200 mL glass reaction vessel and made up to 100.0 mL with deionised water. All solutions were made 6.25 mM with respect to Ca^{2+}, 10.2 mM with respect to CO$_3^{2-}$, 60.7 mM with respect to NaCl, 4.3 mM with respect to K$^+$, 2.7 mM with respect to NH$_4^+$ and 11.4 mM with respect to SO$_4^{2-}$. The test solutions were acidified with three drops of concentrated HCl prior to pH adjustment to 10.0 with dropwise addition of 10 M and/or 1 M NaOH, with constant stirring using a magnetic stirrer. A 5 minute period was allowed for pH equilibration at pH 10.0. A 10 mL sample of the pH 10 solution was taken and filtered through a 0.45 micron cellulose acetate filter after the 5 minute equilibration period (t=0 sample). 0.9 g of seed material (CaCO$_3$ or CaHPO$_4$) was added to the remaining 90 mL of pH 10.0 solution, and samples were taken and filtered through 0.45 micron cellulose acetate filters after 15 minutes. The pH was monitored and kept at 10.0 for the duration of the trial. Control runs identical to the above procedure except for the calcium carbonate seed addition were also performed.

Table 1: Parameter settings for the 3 x 2^3 full factorial seeded precipitation experiments (mM) using no seed, 10 g/L $CaCO_3$ seed, or 10 g/L $CaHPO_4$ seed at pH 10.0.

Parameter	Low	High
Mg^{2+}	7.6	15.2
HPO_4^{2-}	0	0.58
CO_3^{2-}	10.2	30.6

Table 2: Ratios of solution magnesium, calcium and carbonate concentrations at start and after unseeded precipitation in the absence of phosphate. LC= low carbonate dose, HC = high carbonate dose, LM = low magnesium dose, HM = high magnesium dose.

Parameter Settings	Pre-unseeded precipitation Solution Conditions		Post-unseeded precipitation Solution Conditions	
	Mg^{2+}:Ca^{2+}ratio	CO_3^{2-}:Ca^{2+}ratio	Mg^{2+}:Ca^{2+}ratio	CO_3^{2-}:Ca^{2+}ratio
LC-LM	1.2	1.6	1.8	1.9
HC-LM	1.2	4.9	3.6	12.9
LC-HM	2.4	1.6	3.0	1.7
HC-HM	2.4	4.9	6.6	11.6

2.2.2 Analyses

Analysis of the filtrate for calcium and magnesium was performed using atomic absorption spectroscopy after acidification, using a nitrous oxide- acetylene flame and 3,000 mg/L potassium addition to mitigate interferences. The precipitate Ca and Mg content was determined from the pre-ASP and post-ASP aqueous concentrations of these metals.

SEM images were taken using a Zeiss Electron Microscope fitted with an Oxford detector ($20mm^2$). Samples of the suspensions were filtered through 0.45 micron filters. The filter membrane was rinsed by pushing 2 mL of deionised water through the membrane using a syringe. The membranes with the filtered solids were dried at 90°C overnight and subsequently coated with carbon for SEM imaging.

2.2.3 Critical nucleus size calculations

The number of monomer in a critical nucleus was calculated using the following equation [16]:$g_c = $

$$\frac{32\pi V_m^2 \delta^3}{3(kTlnS_a)^3} \tag{1}$$

Where V_m = Volume of monomer (m^3/molecule), δ = Interfacial energy (J/m^2), k = Boltzman Constant ($J/°K$), T = temperature (°K), and S_a = degree of supersaturation. A value of 6.13×10^{-29} was used for the V_m for $CaCO_3$ [16]. The interfacial energy was estimated using the following empirical relationship [16]:

$$\delta = 2028.4 \times [Mg^{2+}] + 68.4 \tag{2}$$

The degree of supersaturation was calculated from the ionic product (IP) and the Ksp of amorphous $CaCO_3$ (9×10^{-7}, [27] according to the following equation:

$$S_a = \left(\frac{IP}{Ksp}\right)^{1/2} \tag{3}$$

3. Results and Discussion

According to the classical theory of homogeneous nucleation, the onset of precipitation is preceded by the formation of clusters. These form when the solution is supersaturated with respect to the precipitating salt. If the size of a cluster exceeds a critical size, a nucleus forms and the subsequent growth of nucleus leads to a visible solid or precipitate. The time interval between the onset of supersaturation and the formation of a cluster of critical size is defined as the induction period, t_{ind}. It has been found that substances such as Mg^{2+} ions and HPO_4^{2-} ions can increase this induction time and thus slow precipitation [9, 20]. Magnesium ions can also increase the critical cluster size [15], thus slowing precipitation or preventing precipitation. The addition of seed material decreases the induction time by increasing the concentration of clusters in the vicinity of the seed surface, thus accelerating the rate of association between clusters and reaching the critical size sooner [28].

3.1 Seeded precipitation experiments

The Mg^{2+}, HPO_4^{2-} and CO_3^{2-} ions content of the tests solutions used in these experiments were chosen to simulate the composition of RO concentrates from phosphate and magnesium-bearing wastewaters and magnesium-bearing groundwaters, and, which exhibit supersaturation with
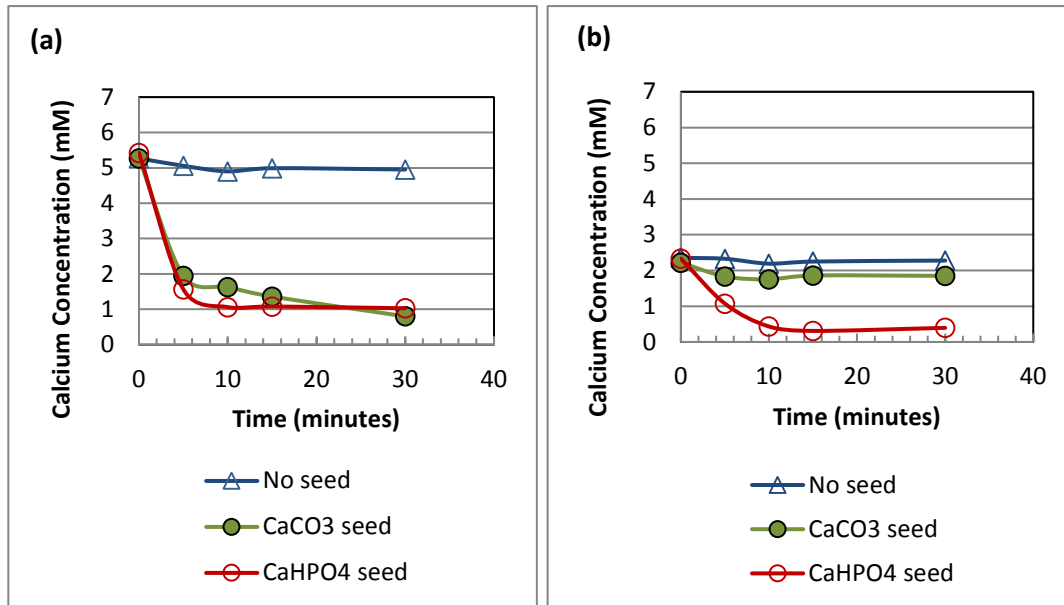
respect to calcium carbonate. The effect of seed type ($CaCO_3$ or $CaHPO_4$) on the rate of calcium precipitation at 15.2 mM Mg at different CO_3 levels is shown in Figure 1. The effect of two different magnesium concentrations and two different carbonate concentrations in the presence and in the absence of phosphate (see Table 1) without seed, with $CaCO_3$ seed or with $CaHPO_4$ seed was investigated. The results after a 15 minute equilibration period are shown in Figure 2 to Figure 4.

Figure 1: Effect of seed type, no HPO_4^{2-} addition, 6.25 mM starting calcium concentration, 15.2 mM starting Mg concentration, (a) 10.2 mM CO_3^{2-}, (b) 30.6 mM CO_3^{2-}.

It can be seen from Figure 1 that the residual calcium concentration after unseeded precipitation is different at the two different carbonate concentrations, and that the addition of seed reduces the induction time from more than 30 minutes (no seed) to less than 5 minutes. The extent of precipitation after seed addition can also be seen to vary under the different test conditions.

3.1.1 Precipitation in the absence of added seed

The effect of simply raising the pH of the solution to 10.0 (i.e., without seed addition) on the precipitation of calcium is shown in Figure 2. Allowing for a calculated 8% experimental error,

unseeded precipitation of calcium in the absence of phosphate (see Figure 2(a)) can be seen to be enhanced by increasing carbonate concentration and inhibited by increasing Mg concentration.

The inhibitory effect of Mg, however, was found to be less at high carbonate (HC) concentrations, suggesting that an increase in bulk carbonate concentration favours Ca adsorption/precipitation over Mg adsorption/precipitation. The inhibitory effect of Mg on the unseeded precipitation of $CaCO_3$ in solution has been well documented [16, 17, 18, 12, 19] and has been attributed to the lengthening of the induction time due to an increase in interfacial tension at the nuclei surface which results in a smaller concentration of coagulated clusters and a larger critical size of nuclei [16].
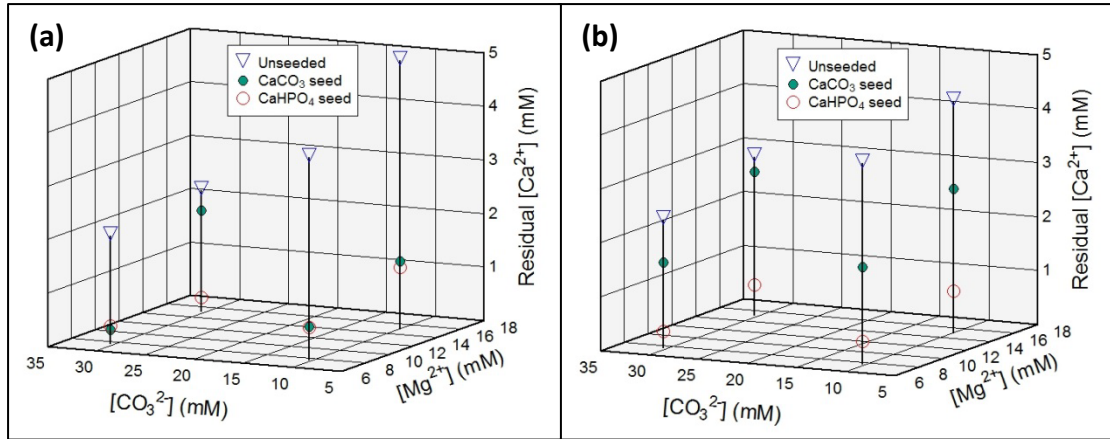
Figure 2: Residual calcium concentration in the absence (a) and in the presence (b) of phosphate at various starting magnesium and carbonate levels
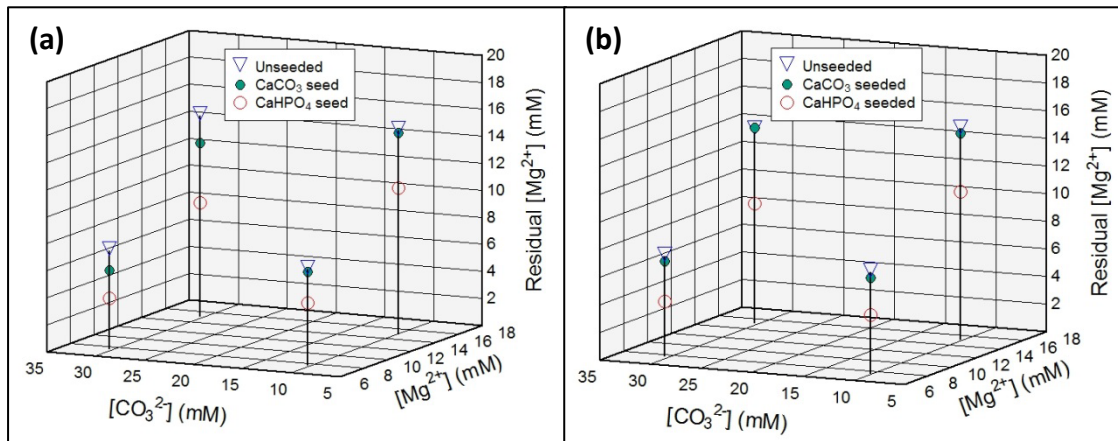

Figure 3: Residual magnesium concentrations in the absence (a) and in the presence (b) of phosphate at various starting magnesium and carbonate levels
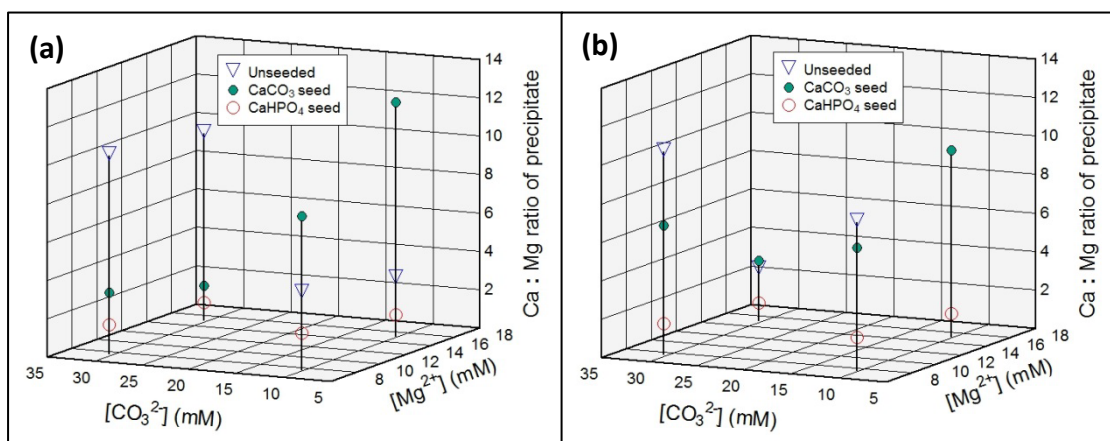

Figure 4: Ca:Mg mole ratio of the precipitate in the absence (a) and in the presence(b) of phosphate (Low carbonate-high Mg unseeded data point off scale – no decrease in Mg concentration detected)

The residual calcium concentration at any given time after chosen test conditions have been achieved depends on the induction period and the critical nucleus size below which precipitation does not take place. The influence of degree supersaturation (S_a) and [Mg] on the resulting interfacial energy (δ) and number of monomers in the critical nucleus size (g_c) was estimated using classical nucleation theory [16] from the no-phosphate unseeded precipitation data shown in Figure 2(a). The results are shown in Table 3.

Table 3: Number of monomers in a critical nucleus, unseeded precipitation

		[Ca] (mM)	[CO$_3$] (mM)	[Mg] (mM)	δ	Sa	g_c
LC base case	No Mg	6.25	10.2	0	0.068	8.4	60
HC base case	No Mg	6.25	30.6	0	0.068	15.8	27
Initial conditions	LC-LM	6.25	10.2	7.6	0.084	8.4	110
	LC-HM	6.25	10.2	15.2	0.099	8.4	183
	HC-LM	6.25	30.6	7.6	0.084	14.6	55
	HC-HM	6.25	30.6	15.2	0.099	14.6	92
Post-unseeded precipitation	LC-LM	3.80	7.1	7.0	0.083	5.5	208
	LC-HM	5.00	8.6	14.8	0.098	6.9	240
	HC-LM	2.00	26.0	7.2	0.083	7.6	124
	HC-HM	2.30	26.2	14.8	0.098	8.1	189

The post-unseeded precipitation residual [Ca] levels in Table 3 can be seen to correlate well with the estimated g_c values – the higher the g_c, the higher the residual [Ca]. This trend is due to the combined effect of Mg on the interfacial energy, and the degree of supersaturation (S_a). Comparison of the low carbonate (LC), no-Mg, base case with the LC initial conditions (before unseeded precipitation has taken place) shows that increasing the [Mg] from zero to 7.6 mM and 15.2 mM at low carbonate condition (10.2 mM) increases the calculated number of monomers in the critical nucleus (g_c) from 60 to 110 and 183 respectively. The subsequent unseeded precipitation reduces the supersaturation from 8.4 to 5.5 and 6.9 respectively and further increases the g_c to 208 and 240 respectively. At the high carbonate condition (HC), the same [Mg] increases gives rise to a similar increase in g_c relative to the HC- no-Mg, base case (27, 55, 92). The subsequent unseeded precipitation reduces S_a from 14.6 to 7.6 and 8.1 respectively, and increases g_c to 124 and 189 respectively.

Comparison of Figure 2(a) and Figure 2(b) shows that phosphate can mildly enhance or inhibit unseeded calcium precipitation, depending on the carbonate level. The presence of phosphate mildly enhanced calcium precipitation at the low carbonate (LC), high magnesium (HM), condition,

and mildly inhibits calcium precipitation at both HC conditions. These effects appear to be counterintuitive as an increase in carbonate level would be expected to decrease the ability of the phosphate anion to compete with the carbonate anion for available calcium surface sites, thereby decreasing the inhibitory effect of phosphate with increasing carbonate concentration. This suggests that the adsorbing phosphate species that interferes with calcium carbonate precipitation is uncharged, as indicated by previous literature studies that show that the inhibitory effect of phosphate can be attributed to the chemisorption of the uncharged aqueous $CaHPO_4$ species [21], which blocks the active calcium carbonate surface sites, preventing or slowing further calcium carbonate deposition.

Magnesium seems to not be involved in the mild inhibitory effect of phosphate at both LC and HC conditions. The magnesium precipitation was found to be largely unaltered by the presence of phosphate (compare Figure 3(a) with Figure 3(b)). Both low carbonate conditions yielded an increase in precipitate Ca:Mg ratio (i.e. less Mg in the precipitate) as a result of phosphate addition (Compare Figure 4(a) with Figure 4(b)), suggesting that phosphate addition can decrease the inhibitory effect of Mg by blocking Mg adsorption sites at these low carbonate conditions. The residual Mg (Figure 3) and the Ca:Mg ratio of the precipitate (Figure 4) were, however, unaltered by phosphate addition at the HC-LM condition. This is consistent with the low inhibitory effect of magnesium at HC-LM condition (see Figure 2(a)). A marked decrease in the precipitate Ca:Mg ratio was observed for the HC-HM experiment on phosphate addition (see Figure 4(b)), suggesting the formation of carbonated apatite and/or magnesium-substituted carbonated apatite [29] under these conditions. The test solutions are expected to be supersaturated with respect to these apatites ($pIAP_{HAP}$ metastable equilibrium solubility (MES) distributions between 110 and 125 [30], $pIAP_{HAP}$ ($Ca_{10}(OH)_2(PO_4)_6$) for the current experiment was 54).

3.1.2 Precipitation in the presence of calcium carbonate seed

The addition of seed to a supersaturated solution is believed to accelerate precipitation due to van der Waals attractive force between the seed and the clusters. This results in a higher concentration of clusters near the surface of the seed than that in the bulk liquid phase, and therefore, the rate of association between clusters is accelerated. Modelling of the effect of seed on the induction time for calcium carbonate precipitation in the absence of impurities using classical nucleation theory has been performed [28]. This effect is, however, influenced by changes to the clusters and to the seed surface brought about by the presence of interfering substances. Further research with a focus on the effects of different seed and the presence of solutes on the cluster concentrations in the vicinity of the seed is warranted.

The addition of 10 g/L $CaCO_3$ seed was found to be effective in lowering the calcium concentration from the unseeded precipitation levels at the LC-LM and the HC-LM conditions (see Figure 2(a)). As expected, increasing the Mg concentration was found to inhibit the seeded precipitation. In contrast to the unseeded precipitation case, however, the inhibitory effect of Mg at the HM condition is greater at the HC concentrations. At the HC-HM condition, the residual calcium concentration was very similar to that of unseeded precipitation, suggesting a high level of inhibition. It appears that conditions with lower driving force for formation of magnesium carbonate, either because of low Mg or low carbonate, allowed the $CaCO_3$ seed to accelerate calcium carbonate precipitation to some degree. The involvement of Mg is confirmed by comparison of Figure 2 with the residual Mg concentration data in Figure 3 which shows that some Mg is being precipitated at the HC conditions. The higher involvement of Mg in the HC-HM situation is also reflected in the lower precipitate Ca:Mg ratio (~2, Figure 4). It is interesting to note, however, that a low precipitate Ca:Mg ratio is not necessarily concomitant with a greater inhibitory effect. The precipitate Ca:Mg ratio was also low for the HC-LM situation (3) where the $CaCO_3$ seed was very effective at removing calcium (Figure 3), suggesting that the HC-LM conditions are conducive to $MgCO_3$ precipitation independently of $CaCO_3$ precipitation while the HC-HM condition is conducive to magnesium adsorption and modification of the seed surface properties leading to inhibition.

According to the cluster coagulation model [16], the induction time for unseeded calcium carbonate precipitation depends on the interfacial tension (surface energy) of the precipitating solid. The adsorption of Mg onto the calcium carbonate surface was found to increase the induction time of calcium carbonate precipitation. This was due to an increase in interfacial tension of the $CaCO_3$ clusters, and a smaller coagulation concentration of clusters and a larger critical size of nuclei, resulting in longer induction time. The cluster coagulation model also revealed that the addition of seed decreased the induction time by allowing a higher concentration of coagulation clusters to be achieved in the region near the seed crystals. The higher coagulation concentration of clusters was attributed to the van der Waals attractive force between the clusters and seed crystals.

The effect of Mg on calcium carbonate seeded precipitation of calcium has recently been studied and it was found that the presence of Mg inhibits calcium carbonate crystal growth [19]. A competitive Langmuir type adsorption model involving Ca^{2+} and Mg^{2+} was found to give a good fit to the crystal growth data, and it was found that the rate of crystal growth depends on the solution Mg:Ca ratio rather than the total Mg concentration. In these constant supersaturation experiments at variable CO_3^{2-}: Ca^{2+} ratios up to 1, as the Mg concentration was increased, the maximum inhibitory effect of Mg was found to occur at solution Mg:Ca ratios above 1. Comparison of this finding with

the current results suggests that the relative quantities of Mg and Ca may also be important determinants of inhibition under the test conditions of the current experiment. The solution Mg:Ca and the CO_3^{2-}: Ca^{2+} ratios for the current experiments are shown in Table 2. It can be seen that the Mg:Ca ratio was 3.6 at the HC-LM condition where very little Mg inhibition was observed, whereas the Mg:Ca ratio was 6.6 at the HC-HM condition where the inhibitory effect of Mg was the greatest. The presence of phosphate was also found to be inhibitory to calcium precipitation using $CaCO_3$ seed, particularly at the HC-LM condition where $CaCO_3$ seed was found to be most effective in the absence of phosphate. The small decrease in residual Mg observed in the absence of phosphate at the HC-LM condition was not observed in the presence of phosphate, suggesting a lower involvement of Mg in the observed inhibitory effect. The lower involvement of Mg was also evident in the precipitate Ca:Mg ratio which was found to increase from 3.2 to 6.7 by the presence of phosphate. It would appear that phosphate, which is believed to adsorb as $CaHPO_{4(aq)}$ [21], adsorbs on the seed or nuclei surface and prevents or hinders the Mg-Ca co-adsorption that is associated with the inhibitory effect of Mg [19]. The adsorption of phosphate on calcium carbonate has been studied using NMR [31] and it has been found that the adsorbing phosphate species form a carbonated apatite-like phase at low surface concentration (3-37 µmole P (sorbed). g^{-1} $CaCO_3$, at pH 7 to 8), and some of this phase was found to be converted to brushite ($CaHPO_4.2H_2O$) at higher surface concentrations (63 µmol. P sorbed g^{-1} $CaCO_3$, pH 7.5). Given the similar available quantities of phosphate and $CaCO_3$ in the current experiment (58 µmole P for every gram of $CaCO_3$) and the high pH of 10, which is conducive to higher phosphate adsorption, it may be speculated that high solution carbonate concentrations facilitate the formation of the carbonated apatite like surface species and phosphate inhibition of seeded calcium precipitation.

The $CaCO_3$ seeded precipitation results presented in the current study suggest that calcium carbonate seeded ASP is limited to waters that do not contain phosphate and conditions that are not conducive to the formation of $MgCO_3$. Municipal wastewaters typically contain phosphorus concentrations between 20 and 50 mg/L (0.8 to 1.6 mM phosphate, [32] and $CaCO_3$ seeded ASP performance would be expected to be severely adversely affected at these phosphate levels. For groundwaters, which typically contain no phosphate and considerable quantities of Mg [33, 34] the key determinant of the suitability of $CaCO_3$ are expected to be the alkalinity of the groundwater and the calcium level relative to the Mg level. Generally, calcium carbonate seeded ASP would be expected to only be suited to RO concentrates from groundwaters with low alkalinity (in excess of the stoichiometric requirement for calcium carbonate precipitation) and/or high Ca levels relative to the Mg levels. Calcium carbonate seeded ASP performance would be expected to be good for RO concentrates from brackish surface waters with relatively low Mg and higher Ca levels, high alkalinity

and little or no phosphate content, as was found in literature studies of calcite seeded ASP for RO concentrates of Colorado River water [5].

3.1.3 Precipitation in the presence of calcium phosphate seed

In the absence of phosphate (Figure 2(a)), seeded precipitation using $CaHPO_4$ seed was found to be as effective as with $CaCO_3$ seed at both LM concentrations, and at the LC-HM concentration, but greatly outperformed $CaCO_3$ seeded precipitation at the HC-HM concentration. This suggests that $CaHPO_4$ may be useful for ASP treatment of RO concentrates from highly carbonated groundwaters such as those in Australian gasfields, and that $CaCO_3$ seed may be the cheaper option for waters with low phosphate and low potential for $MgCO_3$ formation. The cost of agricultural grade $CaCO_3$ is approximately half the cost of agricultural grade $CaHPO_4$.

Comparison of Figure 2(a) with the residual Mg concentration data in Figure 3(a) shows that Mg is being precipitated at all conditions tested, but particularly at the HC-HM condition in the presence of $CaHPO_4$ seed. The precipitate Ca:Mg ratio data (Figure 4(a)) shows that the two metals are being precipitated in approximately equal quantities in the case of $CaHPO_4$ seeded precipitation. The ratio of Ca:Mg in the precipitate (Figure 4) was found to be approximately 1.5 and 1 for the HC-LM and HC-HM conditions respectively. The presence of phosphate did not significantly affect the quantity of Mg precipitated with the calcium (compare Figure 3(a) and Figure 3(b)), and the Ca:Mg ratio remained close to 1 (Figure (b)). The close to equal quantities of Ca and Mg in the precipitate suggests that a mixed metal carbonate is being formed, i.e. dolomite, $CaMg(CO_3)_2$ or, coincidentally, equal quantities of $CaCO_3$ and $MgCO_3$.

The use of $CaHPO_4$ seed can also be seen to avoid the inhibitory effect of phosphate. Comparison of the Figure 2(a) with Figure 2(b) shows that the inhibitory effect that was seen to be very pronounced with $CaCO_3$ seeded precipitation was not evident. The presence of phosphate was found to mildly enhance calcium removal at the low carbonate concentration, and mildly inhibit calcium removal at the HC-HM concentration. These results are consistent with the surface precipitation of calcium phosphate on the calcium phosphate seed and/or on the $CaCO_3$ nuclei thus preventing their growth.

The better performance of $CaHPO_4$ seed than $CaCO_3$ seed at the HC-HM condition may be attributable to the heterocoagulation of the positively charged calcium phosphate [35] and the negatively charge calcium carbonate [36] or dolomite [37] clusters at pH 10, resulting in a shorter induction time for calcium carbonate precipitation due to a higher concentration of clusters in the vicinity of the seed surface. This is a similar scenario to that proposed by [16] for the effect of $CaCO_3$ seed crystals where the reduction in induction period of calcium carbonate precipitation is believed

to be caused by the higher coagulation concentration of clusters in the region near the seed surface. In this situation, however, the seed and the clusters have like charge and the driving force for coagulation is only from the van der Waals attractive force between the clusters and seeds [16]. The different surface charge of $CaCO_3$ and $CaHPO_4$ would also be expected to influence the susceptibility to interference from magnesium. The positively charged magnesium species present at pH 10 (Mg^{2+}, $Mg(OH)^+$) are more readily adsorbed onto the negative $CaCO_3$ surface than the positive $CaHPO_4$ surface, thus blocking surface adsorption sites for calcium adsorption and precipitation on $CaCO_3$ seed. Since seeded precipitation is a surface chemical phenomenon and the two different seed material were dosed at the same rate of 10 g/L, the higher surface area of the $CaHPO_4$ seed (2.3 m^2/g) than of $CaCO_3$ seed (0.96 m^2/g) may also have contributed to the better performance of $CaHPO_4$.

It is noteworthy that the heterocoagulation of seed and nuclei clusters can also be induced by adsorption of surfactants that adsorb on both the seed and the nuclei surface, thus rendering both hydrophobic. Such an approach has been seen in the literature where the adsorption of asphaltenes (surface active amphipathic crude oil components) onto clay particles was found to enhance the particle's ability to act as seed for calcium carbonate precipitation [38] This approach may be useful in the development of less expensive and more effective seed materials for calcium precipitation from municipal wastewater.

The results of Vralstad et al. [38], and the stark difference in performance of calcium carbonate and calcium phosphate seed materials seen in previous studies on municipal wastewater [2 and in the current study on simulated wastewater, point to the prospect of further studies to investigate the feasibility of modification of the surface properties of calcium carbonate seed to improve its performance as seed by making them more like those of calcium phosphate, e.g., by making the calcium carbonate seed less negatively (or positively) charged by adsorption of cationic species (e.g., Al^{3+}, $Al(OH)^{2+}$, $Al(OH)_2^+$), or to develop novel seed materials of the desired surface properties from inexpensive materials. The possibility also exists, as has been demonstrated in literature, of improving the performance of calcium carbonate by rendering the surface hydrophobic via surfactant adsorption.
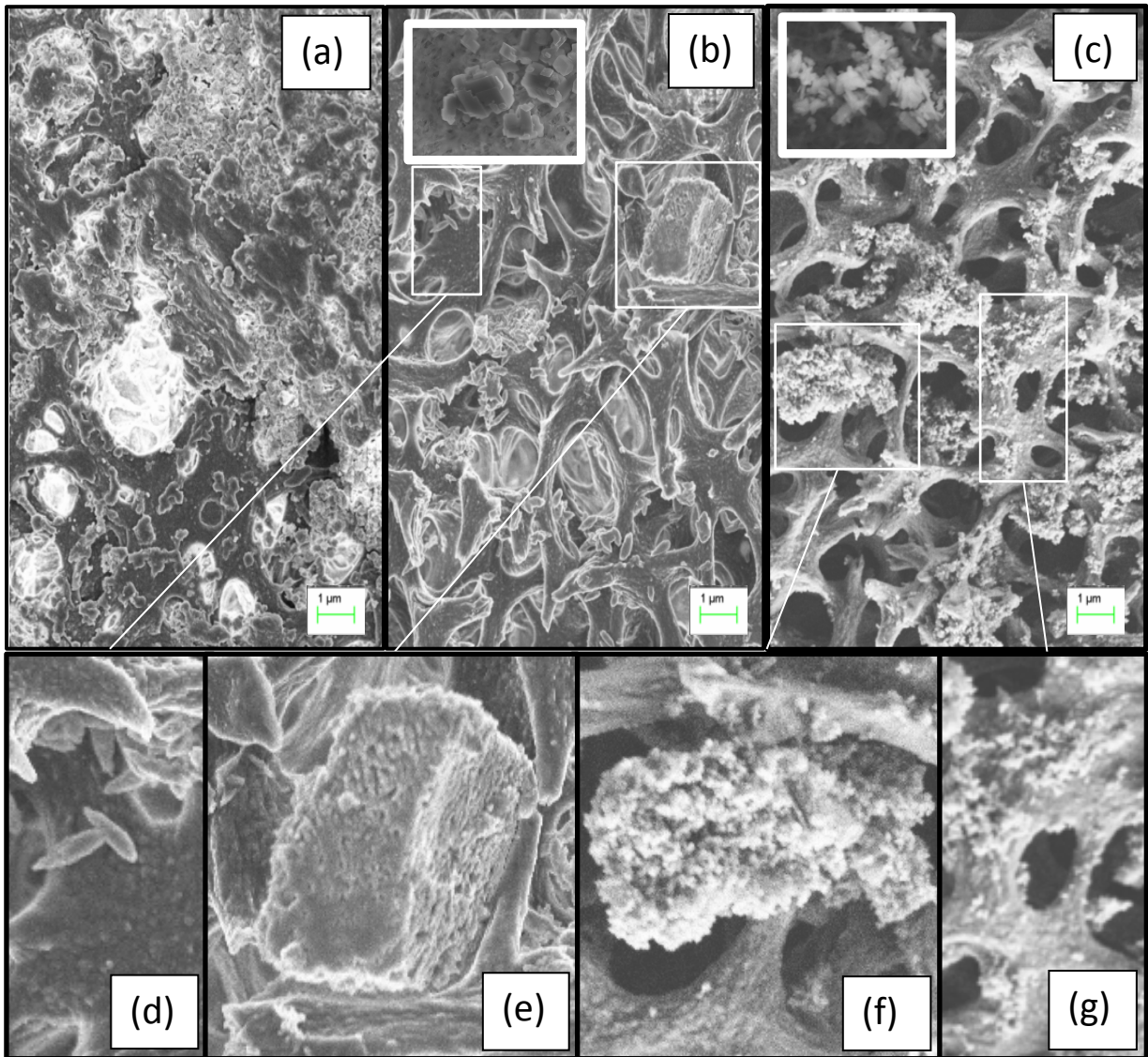
Figure 5: SEM image of the solid produced at high Mg (15.2 mM) and high CO_3 (30.6 mM), in the presence of phosphate (56 mg/L) on a cellulose acetate 0.45 micron filter used to remove the solids from the mother liquor : (a) in the absence of added seed; (b) in the presence of $CaCO_3$ seed; (c) in the presence of $CaHPO_4$ seed; (d) detail from image 5(b) showing calcium aragonite-like crystals, (e) detail from image 5(b) showing cubic calcium carbonate seed crystal with thin layer of precipitate; (f) detail from image 5(c) showing what appears to be precipitated material on $CaHPO_4$ seed; (g) detail of image 5(c) showing traces of fine precipitate on the membrane material. The inserts in images 5(b) and 5(c) are low magnification images of $CaCO_3$ seed and $CaHPO_4$ seed respectively.

3.2 Morphology of precipitate in the presence and in the absence of seed

The SEM image of the solid produced at the HC-HM concentration (Figure 5) shows that the calcium carbonate particles produced in the absence and in the presence of the two different seeds are very different. In the absence of seed (Figure 5(a)) the precipitated amorphous calcium carbonate formed irregular shaped flake-like structures of approximately 0.1 – 0.2 micron in diameter on drying.

The particles seen in the solid produced from the $CaCO_3$ seed experiment, however, are very different (Figure 5(b)). A number of spindle-like structures that are approx. 0.5 micron in length can be seen (see Figure 5(d)). These resemble the spindle-like structures of aragonite crystals that are favoured in the presence of magnesium (Park 2008). These particles appear to have formed independently of the seed, and comparison of these to the rhombus shape of the added $CaCO_3$ seed shown in the Figure 5(e) and in the insert of Figure 5(b) confirms that they are not the original seed material. These images suggest that the amorphous calcium carbonate precipitated before $CaCO_3$ seed addition is converted to aragonite during the 12 hour drying period and that the layer of material on the seed is responsible for the poor seeded precipitation observed in the experiments (see Figure 2). Closer inspection of the calcite crystal in Figure 5(d) shows that the surface of the calcite crystal appears to be covered with a thin layer of material that softens the sharp edges of the crystal. The appearance of the $CaCO_3$ seed is consistent with what would be expected if a thin layer of material forms on the surface of the seed and blocks further crystal growth.

The appearance of the particles formed in the presence of $CaHPO_4$ (Figure 5(c)) is different to that in the absence of seed and in the presence of $CaCO_3$. The particles are much smaller and they form large compact aggregates. Comparison of these to the shape of the added seed shown in the Figure 4(c) insert confirms that they are not the original seed material. Closer inspection of one of these aggregates (Figure 5(f)) shows what appears to be the sharp edge of an underlying $CaHPO_4$ seed, covered with a layer of precipitated material. This image is consistent with what would be expected from the heterocoagulation of the $CaHPO_4$ seed with the calcium carbonate nuclei.

4. Summary and Conclusions

The effect of magnesium and phosphate at various carbonate concentrations on the seeded precipitation of calcium was studied. It was found that $CaCO_3$ seeded ASP is vulnerable to interferences from magnesium and phosphate. The interference by magnesium was found to greatest in the presence of high carbonate concentration, suggesting that this interference involves the formation of $MgCO_3$ on the seed surface or on the $CaCO_3$ nuclei.

The addition of phosphate ion was found to decrease the effectiveness of calcium precipitation using $CaCO_3$ seed under all test conditions, suggesting the adsorption of calcium phosphate onto the newly formed calcium carbonate nuclei thus preventing their growth. ASP using $CaCO_3$ seed may, therefore, not be suitable for RO concentrates from municipal wastewaters as these may contain interfering phosphate levels (if the phosphate is not removed during coagulation pre-treatment). For groundwaters, which typically contain no phosphate and considerable quantities of Mg, calcium carbonate seeded ASP would be expected to be effective at low alkalinity (in excess of the

stoichiometric requirement for calcium carbonate precipitation) and/or high Ca levels relative to the Mg levels. For surface waters, which generally would be expected to have low phosphate levels, $CaCO_3$ seeded ASP performance would be expected to be good at relatively low Mg and higher Ca levels and high alkalinities.

In the absence of phosphate, seeded precipitation using $CaHPO_4$ seed was found to be as effective as with $CaCO_3$ seed at both low magnesium concentrations, and at the low carbonate-high magnesium concentration, but greatly outperformed $CaCO_3$ seeded precipitation at the high carbonate-high magnesium concentration where inhibition was the greatest for $CaCO_3$ seeded precipitation. This suggests that $CaHPO_4$ may be useful for ASP treatment of RO concentrates from highly carbonated groundwaters such as those in Australian gas fields.

In the presence of phosphate, $CaHPO_4$ seeded precipitation was found to be more effective than $CaCO_3$ seed under all conditions tested, particularly at HC-HM conditions where $CaCO_3$ seeded precipitation was ineffective. This confirms previous studies with this seed material that showed it to be an effective, albeit more expensive, option for ASP treatment of wastewater that contains phosphate.

SEM images of the seed particles after seeded precipitation under conditions where $CaCO_3$ seeded precipitation was ineffective showed $CaCO_3$ seeds that appeared to be covered with a thin layer of precipitate, and a number of small aragonite-like crystals that appear to have formed independently of the seed. In contrast to this inhibited crystal growth system of $CaCO_3$ seeded precipitation, SEM images of the solid formed after $CaHPO_4$ seeded precipitation showed seed that had a thick covering of very small particles, as would be expected from the favourable conditions for heterocoagulation of $CaHPO_4$ seed with $CaCO_3$ nuclei.

The results presented in this paper elucidate the conditions under which $CaCO_3$ seeded precipitation may be employed, and point to further areas of research into the ASP treatment of concentrates resulting from RO treatment of magnesium and phosphate-bearing waters. These results also point to complex interactions between seed and solution components that warrant more fundamental studies to give a clearer understanding of the mechanisms involved.

References

[1] C.J. Gabelich, M.D. Williams, A. Rahardianto, J.C. Franklin, Y. Cohen, High-recovery reverse osmosis desalination using intermediate chemical demineralization, Journal of Membrane Science 301 (2007) 131–141.

[2] P. Sanciolo, E. Ostarcevic, P. Atherton, G. Leslie, T. Fane, Y. Cohen, M. Payne, S. Gray, Enhancement of reverse osmosis water recovery using interstage calcium precipitation, Desalination 295 (2012) 43–52.

[3] B. C. McCool, A. Rahardianto, Y. Cohen, Antiscalant removal in accelerated desupersaturation of RO concentrate via chemically-enhanced seeded precipitation (CESP), Water Research 46 (2012) 4261-4271.

[4] A. Venkatesan, P.C. Wankat, Simulation of ion exchange water softening pretreatment for reverse osmosis desalination of brackish water, Desalination 271 (2011) 122–131.

[5] A. Rahardianto, J. Gao, C.J. Gabelich, M.D. Williams, Y. Cohen, High recovery membrane desalting of low-salinity brackish water: Integration of accelerated precipitation softening with membrane RO, Journal of Membrane Science 289 (2007) 123–137.

[6] D. Qu, J. Wang, L. Wang, D. Hou, Z. Luan, B. Wang, Integration of accelerated precipitation softening with membrane distillation for high-recovery desalination of primary reverse osmosis concentrate, Separation and Purification Technology 67 (2009) 21–25.

[7] S.S.Salvador Cob, C. Beaupin, B. Hofs, M.M. Nederlof, D.J.H. Harmsen, E.R. Cornelissen, A. Zwijnenburg, F.E. Genceli Guner, G.J. Witkamp, Silica and silicate precipitation as limiting factors in high-recovery reverse osmosis operations, Journal of Membrane Science 423–424 (2012) 1–10.

[8] A. Subramani, E. Cryer, L. Liu, , S. Lehman, R.Y. Ning, , J.G. Jacangelo, Impact of intermediate concentrate softening on feed water recovery of reverse osmosis process during treatment of mining contaminated groundwater, Separation and Purification Technology 88 (2012) 138–145.

[9] P. Sanciolo, L. Zou, S. Gray, G. Leslie, D. Stevens. Accelerated seeded precipitation pre-treatment of municipal wastewater to reduce scaling, Chemosphere 72 (2008) 243–249.

[10] Y.P. Lin, P.C. Singer, Effects of seed material and solution composition on calcite precipitation, Geochimica et Cosmochimica Acta, Vol. 69, No. 18, (2005) pp. 4495–4504.

[11] M.G. Lioliou, C.A. Paraskeva, P.G. Koutsoukos, A.C. Payatakes, Heterogeneous nucleation and growth of calcium carbonate on calcite and quartz, Journal of Colloid and Interface Science, 308 (2007) 421–428.

[12] T. Chen, A. Neville, M. Yuan, Influence of Mg^{2+} on $CaCO_3$ formation—bulk precipitation and surface deposition, Chemical Engineering Science 61 (2006) 5318 – 5327.

[13] T. Waly, M.D Kennedy, G.J. Witkamp, G. Amy, J.C. Schippers, The role of inorganic ions in the calcium carbonate scaling of seawater reverse osmosis systems Desalination 284 (2012) 279–287.

[14] W.K. Park, S.J. Ko, S.W. Lee, K.H. Cho, J.W. Ahn, C. Han, Effects of magnesium chloride and organic additives on the synthesis of aragonite precipitated calcium carbonate, Journal of Crystal Growth 310 (2008) 2593–2601.

[15] H. Tang, J. Yu, X. Zhao, Controlled synthesis of crystalline calcium carbonate aggregates with unusual morphologies involving the phase transformation from amorphous calcium carbonate, Materials Research Bulletin 44 (2009) 831–835.

[16] C. Y. Tai, W. C. Chien, Interpreting the effects of operating variables on the induction period of $CaCl_2$–Na_2CO_3 system by a cluster coagulation model, Chemical Engineering Science 58 (2003) 3233 – 3241.

[17] E. Loste, R.M. Wilson, R. Seshadri, F.C. Meldrum, The role of magnesium in stabilising amorphous calcium carbonate and controlling calcite morphologies, Journal of Crystal Growth 254 (2003) 206–218.

[18] A.J. Xie, Y.H. Shen, X.Y. Li, Z.W. Yuan, L.G. Qiu, C.Y. Zhang, Y.F.. Yang, The role of Mg^{2+} and Mg^{2+}/amino acid in controlling polymorph and morphology of calcium carbonate crystal, Materials Chemistry and Physics 101 (2007) 87–92.

[19] Y.P. Lin, P.C. Singer, Effect of Mg^{2+} on the kinetics of calcite crystal growth, Journal of Crystal Growth 312 (2009) 136–140.

[20] A. Katsifaras, N. Spanos, Effect of inorganic phosphate ions on the spontaneous precipitation of vaterite and on the transformation of vaterite to calcite, Journal of Crystal Growth 204 (1999) 183 -190.

[21] Y.P. Lin, P.C. Singer, Inhibition of calcite precipitation by orthophosphate: Speciation and thermodynamic considerations, Geochimica et Cosmochimica Acta. 70 (2006) 2530–2539.

[22] E.P.A. Van Langerak, H. Ramaekers, J. Wiechers, A.H.M. Veeken, H.V.M. Hamelers, and G. Lettinga, Impact of location of $CaCO_3$ precipitation on the development of intact anaerobic sludge, Wat. Res. Vol. 34, No. 2, (2000) pp. 437-446.

[23] L.J. Plant, W.A. House, Precipitation of calcite in the presence of inorganic phosphate, Colloids and Surfaces A: Physicochemical and Engineering Aspects 203 (2002) 143–153.

[24] S. Bentov, S. Weil, L. Glazer, A. Sagi, A. Berman, Stabilization of amorphous calcium carbonate by phosphate rich organic matrix proteins and by single phosphoamino acids, Journal of Structural Biology 171 (2010) 207–215.

[25] T. Chen, A. Neville, M. Yuan, Assessing the effect of Mg^{2+} on $CaCO_3$ scale formation–bulk precipitation and surface deposition, Journal of Crystal Growth 275 (2005) e1341–e1347.

[26] P. Sanciolo, E. Ostarcevic, P. Atherton, G. Leslie, T. Fane, Y. Cohen, M. Payne, and S.R. Gray, Effect of Reverse Osmosis Concentrate Composition on Effectiveness of Seeded Precipitation Removal of Scale Precursor Ions to Enhance Water Recovery. In: AWA Membranes and Desalination Speciality IV Conference, 9-11 February, 2011, Surfers Paradise, Queensland, Australia.

[27] J. R. Clarkson, T. J. Price, and C. J. Adams, Role of metastable phases in the spontaneous precipitation of calcium carbonate. J. Chem. Soc. Faraday Trans., 88(2) (1992) 243-249.

[28] C.Y. Tai, W.C. Chien, and J.P. Hsu, Induction Period of $CaCO_3$ Interpreted by the Smoluchowski's Coagulation Theory, AIChE Journal Vol. 51, No. 2 (2005) 480-486.

[29] T.S. Sampath Kumar, I. Manjubala, J. Gunasekaran, Synthesis of carbonated calcium phosphate ceramics using microwave irradiation, Biomaterials 21 (2000) 1623-1629.

[30] A. Chhettry, Z. Wang, J. Hsu, J.L. Fox, A.A. Baig, A.M. Barry, H. Zhuang, M, Otsuka, and W.I. Higuchi, Metastable Equilibrium Solubility Distribution of Carbonated Apatite as a Function of Solution Composition, Journal of Colloid and Interface Science 218 (1999) 57–67.

[31] Z.R. Hinedy, S. Goldberg, A.C. Chang, and J.P. Yesinowski, A ^{31}P and ^{1}H MAS NMR study of phosphate sorption onto calcium carbonate, Journal of Colloid and Interface Science, Vol. 153. No. 1, (1992) 141-160.

[32] A.T.K. Tran, Y. Zhang, J.Y. Lin, P. Mondal, W. Ye, B. Meesschaert, L. Pinoy, B. Van der Bruggen, Phosphate pre-concentration from municipal wastewater by selectrodialysis: Effect of competing components, Separation and Purification Technology 141 (2015) 38–47.

[33] A.S. Sanchez, I.B.R. Nogueira, R.A. Kalid, Uses of the reject brine from inland desalination for fish farming, Spirulina cultivation, and irrigation of forage shrub and crops, Desalination 364 (2015) 96–107.

[34] S.Y. Lee, R.J. Gilkes, Groundwater geochemistry and composition of hardpans in southwestern Australian regolith, Geoderma 126 (2005) 59–84.

[35] J.C. Liu, W. Wanthi, C.J. Chang, Precipitation flotation of phosphate from water, Colloids and Surfaces A: Physicochem. Eng. Aspects 347 (2009) 215–219.

[36] I. Sondi, J. Biscan, N. Vdovic, S.D. Skapin, The electrokinetic properties of carbonates in aqueous media revisited, Colloids and Surfaces A: Physicochem. Eng. Aspects 342 (2009) 84–91.

[37] O.S. Pokrovski, J. Schott, and F. Thomas, Dolomite surface speciation and reactivity in aquatic systems, Geochimica et Cosmochimica Acta, Vol. 63, No. 19/20, (1999) 3133–3143.

[38] T. Vralstad, M. Fossen, J. Sjoblom, and P. Randhol, Influence of Interfacial Tension on Seeded Calcium Carbonate Scale Precipitation: Effect of Adsorbed Asphaltenes, Journal of Dispersion Science and Technology, 29 (2008) 440–446.